Infectious Disease Modelling 7 (2022) 430–447

Contents lists available at ScienceDirect

Infectious Disease Modelling

journal homepage: www.keaipublishing.com/idm

Time-dependent force of infection and effective reproduction ratio in an age-structure dengue transmission model in Bandung City, Indonesia

Juni Wijayanti Puspita [a, *], Muhammad Fakhruddin [b], Nuning Nuraini [c], Edy Soewono [c]

[a] Doctoral Program of Mathematics, Faculty of Mathematics and Natural Sciences, Institut Teknologi Bandung, Jl. Ganesha, 10, Bandung, 40132, Jawa Barat, Indonesia
[b] Department of Mathematics, Faculty of Military Mathematics and Natural Sciences, The Republic of Indonesia Defense University, IPSC Area, Sentul, Bogor, 16810, Indonesia
[c] Department of Mathematics, Faculty of Mathematics and Natural Sciences, Institut Teknologi Bandung, Jl. Ganesha, 10, Bandung, 40132, Jawa Barat, Indonesia

ARTICLE INFO

Article history:
Received 24 December 2021
Received in revised form 7 June 2022
Accepted 4 July 2022
Available online 11 July 2022
Handling editor: Dr HE DAIHAI HE

Keywords:
age structure model
dengue transmission
effective reproduction ratio
force of infection

ABSTRACT

Dengue virus infection is a leading health problem in many endemic countries, including Indonesia, characterized by high morbidity and wide spread. It is known that the risk factors that influence the transmission intensity vary among different age groups, which can have implications for dengue control strategies. A time-dependent four – age structure model of dengue transmission was constructed in this study. A vaccination scenario as control strategy was also applied to one of the age groups. Daily incidence data of dengue cases from Santo Borromeus Hospital, Bandung, Indonesia, from 2014 to 2016 was used to estimate the infection rate. We used two indicators to identify the changes in dengue transmission intensity for this period in each age group: the annual force of infection (FoI) and the effective reproduction ratio based on a time-dependent transmission rate. The results showed that the yearly FoI of children (age 0–4 years) increased significantly from 2014 to 2015, at 10.08%. Overall, the highest FoI before and after vaccination occurred in youngsters (age 5–14 years), with a FoI of about 6% per year. In addition, based on the daily effective reproduction ratio, it was found that vaccination of youngsters could reduce the number of dengue cases in Bandung city faster than vaccination of children.

1. Introduction

Dengue is an arbovirus that belongs to the genus Flavivirus (family *Flaviridae*) and is transmitted by female mosquitoes carrying the dengue virus (Tang et al., 2017). There are four widely known dengue serotypes, namely DENV–1, DENV–2, DENV–3, and DENV–4 (Yip et al., 2022). All of the serotypes are found in Indonesia (Sasmono et al., 2018). However, after

* Corresponding author.
E-mail address: juni.wpuspita@yahoo.com (J.W. Puspita).
Peer review under responsibility of KeAi Communications Co., Ltd.

https://doi.org/10.1016/j.idm.2022.07.001

more than fifty years, a fifth serotype (DENV−5), which was recently found in the forests of Sarawak, Malaysia, has been reported in October 2013 (Mustafa et al., 2015). The virus infections have varied clinical manifestations, ranging from asymptomatic infection to severe clinical symptoms such as dengue shock syndrome. One of the risk factors that influence the clinical manifestations is age (Egger & Coleman, 2007). Thai et al. (Thai et al., 2011) states that higher age groups, such as adolescents and young adults, are more likely to develop symptomatic dengue than younger individuals, such as primary school children. Therefore, the age factor not only plays a key role in characterizing the risks of clinical attack and disease severity (Thai et al., 2011) but also determines the best strategy for preventing, treating, and controlling the spread of dengue infection.

Dengue transmission in Indonesia can be categorized as hyper-endemic (Tam et al., 2018). Demographic changes, that is, changes in birth and death rates, have most probably contributed to the upward shift in the age range among dengue hemorrhagic fever (DHF) cases in Indonesia (Karyanti et al., 2014). Karyanti et al. (Karyanti et al., 2014) reported that the highest incidence of DHF in Indonesia from 1968 to 1998 occurred in children aged 5–14 years. However, since 1999, the highest incidence of DHF has shifted towards older age groups (age above 15 years). Meanwhile, incidence in children aged under five years has remained relatively low and stable (Karyanti et al., 2014). In addition, Prayitno et al. (Prayitno et al., 2017) revealed that more than 80% of children aged ten years or over had experienced dengue infection at least once. They even reported that the constant force of primary infection was 13.1% per year in dengue-naive children aged 1–18 years (Prayitno et al., 2017). Further, more than half of children in Indonesia had been exposed to more than one dengue virus serotype, which indicates the intensity of transmission in children, often associated with severe clinical manifestations (Sasmono et al., 2018). Using the same data sample as Prayitno et al. (Prayitno et al., 2017) and Sasmono et al. (Sasmono et al., 2018), Tam et al. (Tam et al., 2018) estimated that each year, 14% of seronegative children have their first infection. They also revealed that the dengue force of infection ranged from 4.3% to 30.0% among urban sub-districts in Indonesia.

Understanding dengue transmission intensity in age groups is essential in determining optimal prevention strategies, such as future vaccine implementation. Moreover, age is the only restriction for vaccine recommendation in countries with high endemicity (Aguiar & Stollenwerk, 2018). Dengvaxia is a tetravalent dengue vaccine produced by Sanofi Pasteur, licensed for trial use in twenty endemic countries, including Indonesia (Thomas & Yoon, 2019). This vaccine is recommended for individuals aged 9–45 years and is still being evaluated in children (Aguiar, Stollenwerk, & Halstead, 2016; Thomas & Yoon, 2019). Takeda Pharmaceutical Company has developed a new tetravalent dengue vaccine candidate, DENVax (TAK 003). It has been reported that the vaccine is efficacious against virologically confirmed dengue fever among healthy children and adolescents aged 4–16 years, regardless of previous dengue exposure (Biswal et al., 2019).

Mathematical modeling can play an important role in considering particular disease control strategies. Several studies have proposed mathematical models to investigate the effects of vaccination programs on the dynamics of the spread of dengue disease. Different aspects of vaccination were considered in these studies, such as constant vaccination of adults and newborns (Bustamam et al., 2018), pulse vaccination (Jan & Xiao, 2019), antibody-depending enhancement (ADE) factors (Kabir & Tanimoto, 2020; Shim, 2019), vaccine efficacy (Aguiar, Mateus, & Stollenwerk, 2016), vaccine coverage levels and cost-effectiveness of different strategies for a vaccination program (Polwiang, 2016; Zeng et al., 2018).

Few studies have developed age-structured compartmental models involving vaccination strategies. Supriatna et al. (Supriatna et al., 2008) presents a two−age structure model, i.e., children and adults, with vaccination of children as control against the spread of dengue transmission. An effective threshold number that is equivalent to the basic reproduction number was shown in that study. This suggests that serological screening of children should be done before vaccination to gain an effective vaccination program. Aguiar et al. (Aguiar, Stollenwerk, & Halstead, 2016) developed a three−age structure model based on Sanofi's recommendation to vaccinate individuals of age 9–45 years in dengue-endemic countries. They investigated the impact of Dengvaxia administration using two vaccination strategies: vaccination of 4 or 20% of seropositive and seronegative individuals, and dengue immune individuals only. The results revealed that to reduce the number of dengue hospitalizations, the vaccination program was most effective when Dengvaxia was given only to individuals that had already been exposed to at least one dengue virus (or seropositive individuals). An age-structure model to evaluate the cost-effectiveness and economic impact of dengue vaccination programs in the Philippines and Yucatán, Mexico, was studied by Shim (Shim, 2016) and Shim (Shim, 2017), respectively. The same as the model in Aguiar et al. (Aguiar, Stollenwerk, & Halstead, 2016), the models in (Shim, 2016, 2017) did not explicitly incorporate mosquitoes into the model. In both studies, the contribution of mosquitoes to dengue transmission was represented by age-dependent transmission rates. These studies found the vaccination cost threshold per individual at which a dengue vaccination program becomes cost-effective.

In the present study, we developed a time-dependent host-vector model for dengue transmission with a four−age structure in the human population. We constructed a time-dependent effective reproduction ratio for measuring the transmission in the population. For measuring the transmission in each age group, we constructed a time-dependent force of infection. Using these two constructions, we analyzed vaccination efficacy in each age group and the whole population.

The rest of this paper is organized as follows. In Section 2, we present dengue cases in Bandung from 2014 to 2016. The time-dependent age structure model in the human population with vaccination as a control strategy is also given in Section 2. We propose the time-dependent force of infection and the effective reproduction ratio. The numerical scheme is presented with a reduction of mosquito dynamics. In Section 3, we present the numerical simulation results, analyses of vaccination efficacy, and discussion. Section 4 provides our conclusions.

2. Material and methods

2.1. Datasets

Bandung, West Java Province, is one of the most populous cities in Indonesia. The West Java Provincial Health Office has reported that Bandung city has the highest number of dengue hemorrhagic fever (DHF) cases in West Java (CNN-Indonesia). The Bandung City Health Office has noted that DHF mostly affects children aged 5–14 years and productive-age individuals (15–44 years) (CNN-Indonesia). This study retrieved dengue case data from daily hospitalization data for the years 2014–2016 from Santo Borromeus Hospital, Bandung. This data is assumed to be half of the total dengue cases in Bandung. We divided the data into four age groups, namely children (0–4 years), youngsters (5–14 years), productive adults (15–60 years), and elders (over 60 years). The normalized data, calculated by multiplying the total number of daily hospitalizations by 100,000 persons and dividing by the total population for the years 2014–2016, are shown in Fig. 1. This representation is commonly used in field observation to measure the number of cases per 100,000 persons. The highest peak in dengue cases was observed in May – June 2016. Fig. 1 also shows that the highest dengue incidence occurred in children and youngsters. Motivated by this fact, the dengue transmission control strategy in this study was focused on providing the most benefit to these two age groups. The irregularity of outbreak and transmission intensity from 2014 to 2016 can also be seen in Fig. 1. Our intention was to analyze the transmission progress by following the transmission characteristics within a yearly period.

2.2. Proposed models and their analysis

2.2.1. Classical model

In this Subsection, we review the host-vector model that was developed by Esteva and Vargas (Esteva & Vargas, 1998), which describes the spread of dengue disease transmission within human and mosquito populations. To fit with the real conditions in the field, we allowed the infection rates to vary over time. The following SIR-UV model is given:

$$\begin{aligned}
\frac{dS(t)}{dt} &= A_h - \frac{\beta_h(t)}{N_h} S(t)V(t) - \mu_h S(t) \\
\frac{dI(t)}{dt} &= \frac{\beta_h(t)}{N_h} S(t)V(t) - (\gamma + \mu_h) I(t) \\
\frac{dR(t)}{dt} &= \gamma I(t) - \mu_h R(t) \\
\frac{dU(t)}{dt} &= A_m - \frac{\beta_v(t)}{N_h} U(t)I(t) - \mu_m U(t) \\
\frac{dV(t)}{dt} &= \frac{\beta_v(t)}{N_h} U(t)I(t) - \mu_m V(t),
\end{aligned} \tag{1}$$

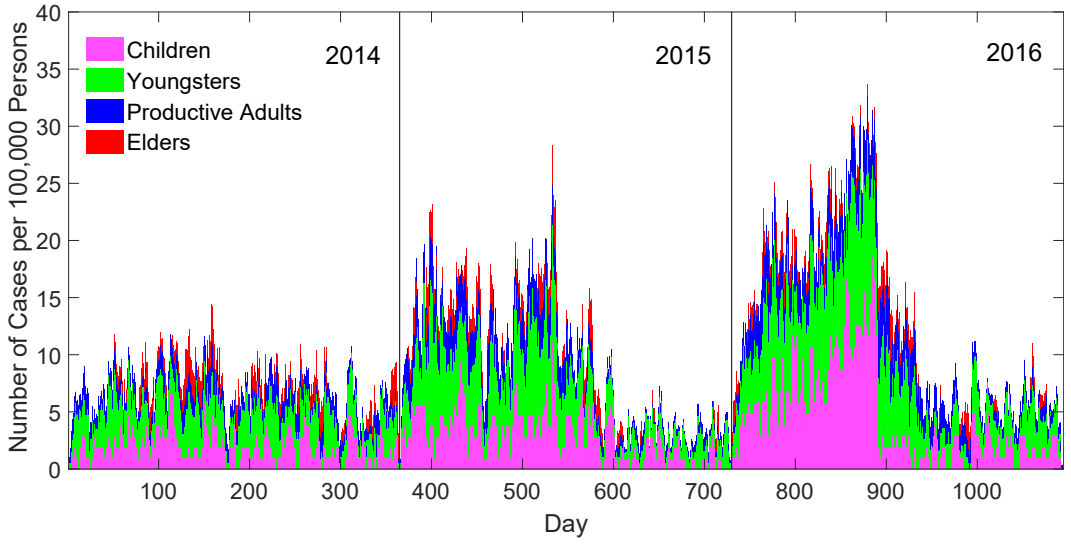

Fig. 1. The number of dengue cases per 100,000 persons between 2014 and 2016.

where $S(t)$, $I(t)$, $R(t)$, $U(t)$, and $V(t)$ represent the number of susceptible humans, infected humans, recovered humans, susceptible mosquitoes, and infected mosquitoes, at time t, respectively. The total human and mosquito populations are defined by $N_h = S(t) + I(t) + R(t)$ and $N_m = U(t) + V(t)$, respectively. Note that $\frac{dN_h}{dt} = 0$ and $\frac{dN_m}{dt} = 0$, which implies that N_h and N_m are constant. The descriptions of the parameters are given in Table 1. For constant infection rates, a non-dimensional quantity called the basic reproduction ratio (R_0) can be derived, which represents the expected number of secondary cases from one primary case in a completely susceptible population during the infection period (Diekmann et al., 2010). The basic reproduction ratio of a classical SIR-UV model is given by:

$$R_0 = \sqrt{\frac{\beta_h \beta_v N_m}{\mu_m(\gamma + \mu_h)N_h}}. \tag{2}$$

As time evolves, the basic reproduction ratio as an endemic indicator in the early infection phase may not be valid for tracking the progress of transmission. The evolution of the indicator can be constructed by defining the effective reproduction ratio (Duijzer et al., 2016; Zhao et al., 2020),

$$R_{eff} = \sqrt{\frac{\beta_h \beta_v U(t) S_h(t)}{\mu_m(\gamma + \mu_h)N_h^2}} = R_0 \sqrt{\frac{S_h(t)}{N_h}\frac{U(t)}{N_m}}. \tag{3}$$

It is natural to adopt and to generalize indicator (3) for model with time-dependent transmission rates as:

$$R_{eff}(t) = \sqrt{\frac{\beta_h(t)\beta_v(t)U(t)S_h(t)}{\mu_m(\gamma + \mu_h)N_h^2}}. \tag{4}$$

Furthermore, we defined the force of infection (FoI) for model (1) as follows:

$$F = \frac{1}{T}\int_0^T \frac{\beta_h(s)V(s)}{N_h}\,ds,$$

which represents the yearly average of probability of a susceptible human being infected per unit time.

2.2.2. Age structure model

In this Subsection, we construct a time-dependent four−age structure model of dengue transmission. Let $S_i(t)$, $I_i(t)$, $R(t)$ denote the number of susceptible, infected, recovered humans, with $i = 1 \ldots 4$ referring to the age structure of children, youngsters, productive adults, and elders, respectively. Meanwhile, U and V denote the number of susceptible and infected mosquitoes, respectively, at time t. We also involve vaccination as an intervention for dengue outbreak control. Based on dengue cases in Bandung, we assume that vaccination is only given to children and youngsters, respectively. The vaccination scenario is implemented only to susceptible individuals. The vaccination parameter for children and youngsters is denoted by

Table 1
Parameter definition and value.

Parameter	Definition	Value	Source
A_h	Human recruitment rate (Day^{-1})	-	(Bandung, 2015, 2016, 2017)
A_m	Mosquito recruitment rate (Day^{-1})	$\mu_m \times N_m$	Assumed
α_1	Transition rate from children to youngsters (Day^{-1})	$\frac{1}{5\times 365}$	-
α_2	Transition rate from youngsters to productive adults (Day^{-1})	$\frac{1}{10\times 365}$	-
α_3	Transition rate from productive adults to elders (Day^{-1})	$\frac{1}{46\times 365}$	-
β_{h_1}	Transmission rate from mosquitoes to children (Day^{-1})	Fitted	-
β_{h_2}	Transmission rate from mosquitoes to youngsters (Day^{-1})	Fitted	-
β_{h_3}	Transmission rate from mosquitoes to productive adults (Day^{-1})	Fitted	-
β_{h_4}	Transmission rate from mosquitoes to elders (Day^{-1})	Fitted	-
β_v	Transmission rate from humans to mosquitoes (Day^{-1})	$2 \times \mu_m$	(Fauzi et al., 2019)
μ_h	Mean mortality (Day^{-1})	$\frac{A_h}{N_h}$	Assumed
μ_m	Natural death rate of mosquitoes (Day^{-1})	$\frac{1}{14}$	(Supriatna et al., 2008)
γ	Recovery rate of infected humans (Day^{-1})	$\frac{1}{14}$	(Supriatna et al., 2008)
θ_1, θ_2	Vaccination parameter with $\theta_j = q\eta, j = 1, 2$, where q is vaccine efficacy and η is vaccination rate (Day^{-1})	$q = 50\%$; $\eta = 1\%$	Assumed based on (Ndii et al., 2020)

$\theta_j = q\eta$ for $j = 1, 2$, where q denotes the vaccine efficacy and η denotes the vaccination rate. Based on the transmission diagram in Fig. 2 and the associated parameters in Table 1, the SIR-UV time-dependent model with a four−age structure is given by:

$$\frac{dX(t)}{dt} = F(X(t)), \tag{5}$$

where $X(t) = (S_1(t), S_2(t), S_3(t), S_4(t), I_1(t), I_2(t), I_3(t), I_4(t), R(t), U(t), V(t))^T$, which can be written in detail as follows:

$$\begin{aligned}
\frac{dS_1(t)}{dt} &= A_h - \frac{\beta_{h_1}(t)}{N_h} S_1(t)V(t) - (\alpha_1 + \mu_h + \theta_1)S_1(t)\\
\frac{dI_1(t)}{dt} &= \frac{\beta_{h_1}(t)}{N_h} S_1(t)V(t) - (\alpha_1 + \gamma + \mu_h)I_1(t)\\
\frac{dS_2(t)}{dt} &= \alpha_1 S_1(t) - \frac{\beta_{h_2}(t)}{N_h} S_2(t)V(t) - (\alpha_2 + \mu_h + \theta_2)S_2(t)\\
\frac{dI_2(t)}{dt} &= \alpha_1 I_1(t) + \frac{\beta_{h_2}(t)}{N_h} S_2(t)V(t) - (\alpha_2 + \gamma + \mu_h)I_2(t)\\
\frac{dS_3(t)}{dt} &= \alpha_2 S_2(t) - \frac{\beta_{h_3}(t)}{N_h} S_3(t)V(t) - (\alpha_3 + \mu_h)S_3(t)\\
\frac{dI_3(t)}{dt} &= \alpha_2 I_2(t) + \frac{\beta_{h_3}(t)}{N_h} S_3(t)V(t) - (\alpha_3 + \gamma + \mu_h)I_3(t)\\
\frac{dS_4(t)}{dt} &= \alpha_3 S_3(t) - \frac{\beta_{h_4}(t)}{N_h} S_4(t)V(t) - \mu_h S_4(t)\\
\frac{dI_4(t)}{dt} &= \alpha_3 I_3(t) + \frac{\beta_{h_4}(t)}{N_h} S_4(t)V(t) - (\gamma + \mu_h)I_4(t)\\
\frac{dR(t)}{dt} &= \sum_{i=1}^{4} \gamma I_i(t) + \theta_1 S_1(t) + \theta_2 S_2(t) - \mu_h R(t)\\
\frac{dU(t)}{dt} &= A_m - \frac{\beta_v(t)}{N_h} \sum_{i=1}^{4} U(t)I_i(t) - \mu_m U(t)\\
\frac{dV(t)}{dt} &= \frac{\beta_v(t)}{N_h} \sum_{i=1}^{4} U(t)I_i(t) - \mu_m V(t),
\end{aligned} \tag{6}$$

with $N_h = \sum_{i=1}^{4}(S_i(t) + I_i(t)) + R(t)$ and $N_m = U(t) + V(t)$ denoting the total human and mosquito populations, respectively. We assume that the human and mosquito populations are constant, i.e., $N_h = \frac{A_h}{\mu_h}$ and $N_m = \frac{A_m}{\mu_m}$. There is no information about mortality for each age structure, thus, the mortality rate is assumed as the mean of mortality with $\mu_h = \frac{A_h}{N_h}$.

2.2.3. Reproduction ratio

In this Subsection, we consider the case of constant infection rates to derive the corresponding reproduction ratios. The disease-free equilibrium of model (6) is given by:

$$\begin{aligned}
DFE = \Big\{ & S_1 = \frac{A_h}{\alpha_1 + \mu_h + \theta_1}, I_1 = 0, S_2 = \frac{A_h\alpha_1}{(\alpha_1 + \mu_h + \theta_1)(\alpha_2 + \mu_h + \theta_2)},\\
& I_2 = 0, S_3 = \frac{A_h\alpha_1\alpha_2}{(\alpha_1 + \mu_h + \theta_1)(\alpha_2 + \mu_h + \theta_2)(\alpha_3 + \mu_h)}, I_3 = 0,\\
& S_4 = \frac{A_h\alpha_1\alpha_2\alpha_3}{\mu_h(\alpha_1 + \mu_h + \theta_1)(\alpha_2 + \mu_h + \theta_2)(\alpha_3 + \mu_h)}, I_4 = 0,\\
& R = \frac{A_h(\alpha_1\theta_2 + (\alpha_2 + \mu_h + \theta_2)\theta_1)}{\mu_h(\alpha_1 + \mu_h + \theta_1)(\alpha_2 + \mu_h + \theta_2)}, U = \frac{A_m}{\mu_m}, V = 0 \Big\}.
\end{aligned}$$

Let J be the Jacobian of I_1, I_2, I_3, I_4, V at the DFE. Following the construction of a next generation matrix (NGM) in (Van den Driessche, 2017), we decompose $J = F - V$, where F consists of new infections (per unit time) coming into each compartment,

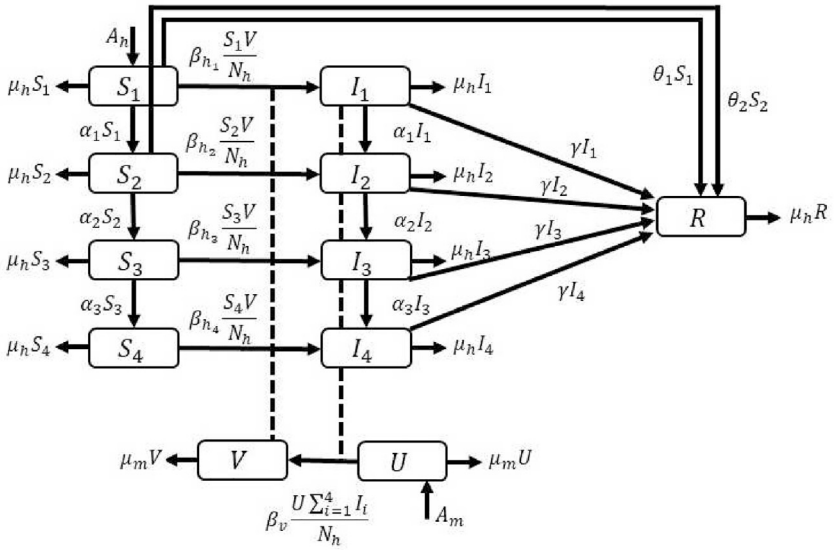

Fig. 2. Schematic diagram of the four – age structure model of dengue transmission. The dash lines represent the contribution of infected mosquitoes or infected humans to dengue transmission.

and V is the transition matrix. The choice of the linear transition matrix V will contribute to different formulations of the reproduction ratio. Here, we select

$$V = \begin{bmatrix} \alpha_1+\mu_h+\gamma & 0 & 0 & 0 & 0 \\ -\alpha_1 & \alpha_2+\mu_h+\gamma & 0 & 0 & 0 \\ 0 & -\alpha_2 & \alpha_3+\mu_h+\gamma & 0 & 0 \\ 0 & 0 & -\alpha_3 & \mu_h+\gamma & 0 \\ 0 & 0 & 0 & 0 & \mu_m \end{bmatrix}.$$

with the corresponding F as:

$$F = \begin{bmatrix} 0 & 0 & 0 & 0 & n_{15} \\ 0 & 0 & 0 & 0 & n_{25} \\ 0 & 0 & 0 & 0 & n_{35} \\ 0 & 0 & 0 & 0 & n_{45} \\ n_{51} & n_{52} & n_{53} & n_{54} & 0 \end{bmatrix},$$

where,

$$\begin{aligned} n_{15} &= \frac{\beta_{h_1}\mu_h}{\alpha_1+\mu_h+\theta_1} \\ n_{25} &= \frac{\beta_{h_2}\alpha_1\mu_h}{(\alpha_1+\mu_h+\theta_1)(\alpha_2+\mu_h+\theta_2)} \\ n_{35} &= \frac{\beta_{h_3}\alpha_1\alpha_2\mu_h}{(\alpha_1+\mu_h+\theta_1)(\alpha_2+\mu_h+\theta_2)(\alpha_3+\mu_h)} \\ n_{45} &= \frac{\beta_{h_4}\alpha_1\alpha_2\alpha_3}{(\alpha_1+\mu_h+\theta_1)(\alpha_2+\mu_h+\theta_2)(\alpha_3+\mu_h)} \\ n_{51} &= n_{52} = n_{53} = n_{54} = \frac{A_m\beta_v\mu_h}{A_h\mu_m}. \end{aligned}$$

With this separation, it is possible to construct the next generation matrix,

$$NGM = FV^{-1} = \begin{bmatrix} 0 & 0 & 0 & 0 & \frac{n_{15}}{\mu_m} \\ 0 & 0 & 0 & 0 & \frac{n_{25}}{\mu_m} \\ 0 & 0 & 0 & 0 & \frac{n_{35}}{\mu_m} \\ 0 & 0 & 0 & 0 & \frac{n_{45}}{\mu_m} \\ \frac{n_{51}}{\mu_h+\gamma} & \frac{n_{52}}{\mu_h+\gamma} & \frac{n_{53}}{\mu_h+\gamma} & \frac{n_{54}}{\mu_h+\gamma} & 0 \end{bmatrix}. \tag{7}$$

We have the characteristic polynomial,

$$P(\lambda) = \lambda^3(p_2\lambda^2 - p_0), \tag{8}$$

where,

$$\begin{aligned} p_2 &= A_h\mu_m{}^2(\alpha_1+\mu_h+\theta_1)(\alpha_2+\mu_h+\theta_2)(\alpha_3+\mu_h)(\mu_h+\gamma) \\ p_0 &= A_m\beta_v\mu_h\Big(\beta_{h_1}\mu_h{}^3 + \big((\theta_2+\alpha_2+\alpha_3)\beta_{h_1} + \alpha_1\beta_{h_2}\big)\mu_h{}^2 + \\ &\quad \big(\alpha_3(\theta_2+\alpha_2)\beta_{h_1} + \alpha_1\big(\alpha_2\beta_{h_3} + \alpha_3\beta_{h_2}\big)\big)\mu_h + \alpha_1\alpha_2\alpha_3\beta_{h_4}\Big). \end{aligned}$$

Thus, we obtain the basic reproduction ratio in explicit form as follows:

$$R_0 = \sqrt{\frac{p_0}{p_2}}. \tag{9}$$

Furthermore, we perform the sensitivity analysis of R_0 as proposed by Tay et al. (Tay et al., 2022) to determine which of the model parameters affect the dynamic behavior of the model (Musa et al., 2020).

Following construction of the corresponding effective reproduction ratio in Eqs. (3) and (4) with time-dependent transmission rates, we obtain

$$R_{eff}(t) = \sqrt{\frac{\beta_v(t)U(t)\left(\sum_{i=1}^{4}\beta_{h_i}(t)S_i(t)\right)}{N_h^2\mu_m(\mu_h+\gamma)}}. \tag{10}$$

Note that the vaccination parameters, θ_j for $j = 1, 2$, do not appear explicitly in Eq. (10). The effect of vaccination is hidden in the dynamics of $S_j(t)$.

2.2.4. Time-dependent reduced age structure model

In this Subsection, we reduce model (6) by freezing the infected mosquito dynamic, see for example in (Götz et al., 2017). This reduction is used with the understanding that mosquito dynamics are much faster than those of humans. Then, from the last two equations in model (6) we have

$$V(t) = \frac{N_v\sum_{i=1}^{4}I_i(t)}{\sum_{i=1}^{4}I_i(t) + \varphi N_h}, \tag{11}$$

where $\varphi = \frac{\mu_m}{\beta_v}$. Thus, we have the following reduced age structure model:

$$\frac{dX(t)}{dt} = F(X(t)), \tag{12}$$

with $X(t) = (S_1(t), I_1(t), S_2(t), I_2(t), S_3(t), I_3(t), S_4(t), I_4(t), R(t))^T$, written in detail:

$$
\begin{aligned}
\frac{dS_1(t)}{dt} &= A_h - \frac{\beta_{h_1}(t)N_v S_1(t)\sum_{i=1}^{4} I_i(t)}{N_h\left(\sum_{i=1}^{4} I_i(t) + \varphi N_h\right)} - (\alpha_1 + \mu_h + \theta_1)S_1(t)\\
\frac{dI_1(t)}{dt} &= \frac{\beta_{h_1}(t)N_v S_1(t)\sum_{i=1}^{4} I_i(t)}{N_h\left(\sum_{i=1}^{4} I_i(t) + \varphi N_h\right)} - (\alpha_1 + \gamma + \mu_h)I_1(t)\\
\frac{dS_2(t)}{dt} &= \alpha_1 S_1(t) - \frac{\beta_{h_2}(t)N_v S_2(t)\sum_{i=1}^{4} I_i(t)}{N_h\left(\sum_{i=1}^{4} I_i(t) + \varphi N_h\right)} - (\alpha_2 + \mu_h + \theta_2)S_2(t)\\
\frac{dI_2(t)}{dt} &= \alpha_1 I_1(t) + \frac{\beta_{h_2}(t)N_v S_2(t)\sum_{i=1}^{4} I_i(t)}{N_h\left(\sum_{i=1}^{4} I_i(t) + \varphi N_h\right)} - (\alpha_2 + \gamma + \mu_h)I_2(t)\\
\frac{dS_3(t)}{dt} &= \alpha_2 S_2(t) - \frac{\beta_{h_3}(t)N_v S_3(t)\sum_{i=1}^{4} I_i(t)}{N_h\left(\sum_{i=1}^{4} I_i(t) + \varphi N_h\right)} - (\alpha_3 + \mu_h)S_3(t)\\
\frac{dI_3(t)}{dt} &= \alpha_2 I_2(t) + \frac{\beta_{h_3}(t)N_v S_3(t)\sum_{i=1}^{4} I_i(t)}{N_h\left(\sum_{i=1}^{4} I_i(t) + \varphi N_h\right)} - (\alpha_3 + \gamma + \mu_h)I_3(t)\\
\frac{dS_4(t)}{dt} &= \alpha_3 S_3(t) - \frac{\beta_{h_4}(t)N_v S_4(t)\sum_{i=1}^{4} I_i(t)}{N_h\left(\sum_{i=1}^{4} I_i(t) + \varphi N_h\right)} - \mu_h S_4(t)\\
\frac{dI_4(t)}{dt} &= \alpha_3 I_3(t) + \frac{\beta_{h_4}(t)N_v S_4(t)\sum_{i=1}^{4} I_i(t)}{N_h\left(\sum_{i=1}^{4} I_i(t) + \varphi N_h\right)} - (\gamma + \mu_h)I_4(t)\\
\frac{dR(t)}{dt} &= \sum_{i=1}^{4} \gamma I_i(t) + \theta_1 S_1(t) + \theta_2 S_2(t) - \mu_h R(t).
\end{aligned}
\tag{13}
$$

Note that for constant transmission rates, this reduction does not change the equilibria and the corresponding reproduction ratios.

We then perform fitting of the reduced model (13) with the incidence data by approaching the first derivative of each compartment using a forward difference approximation for $t = 0 \ldots T-1$ and $\Delta t = 1$, as introduced by Chen et al. (Chen et al., 2020). Furthermore, we approximate $\beta_{h_i}(t)$ from smoothed infected data, $\hat{I}_i(t)$, for $i = 1 \ldots 4$ as follows:

$$
\beta_{h_i}(t) \approx \frac{N_h}{S(t)V(t)}\left(\hat{I}_i(t+1) - (1 - \alpha_i - \mu_h - \gamma)\hat{I}_i(t) - \alpha_{i-1}\hat{I}_{i-1}(t)\right),
\tag{14}
$$

Table 2
Birth and total population data of Bandung (Bandung, 2015, 2016, 2017).

Age Structure	Number of Birth A_h			Total Population (N_{h_i})		
	2014	2015	2016	2014	2015	2016
Children	20090	22900	21847	105286	106578	102883
Youngsters	-	-	-	184804	188079	182947
Productive Adults	-	-	-	855507	858414	861993
Elders	-	-	-	89803	87663	97487

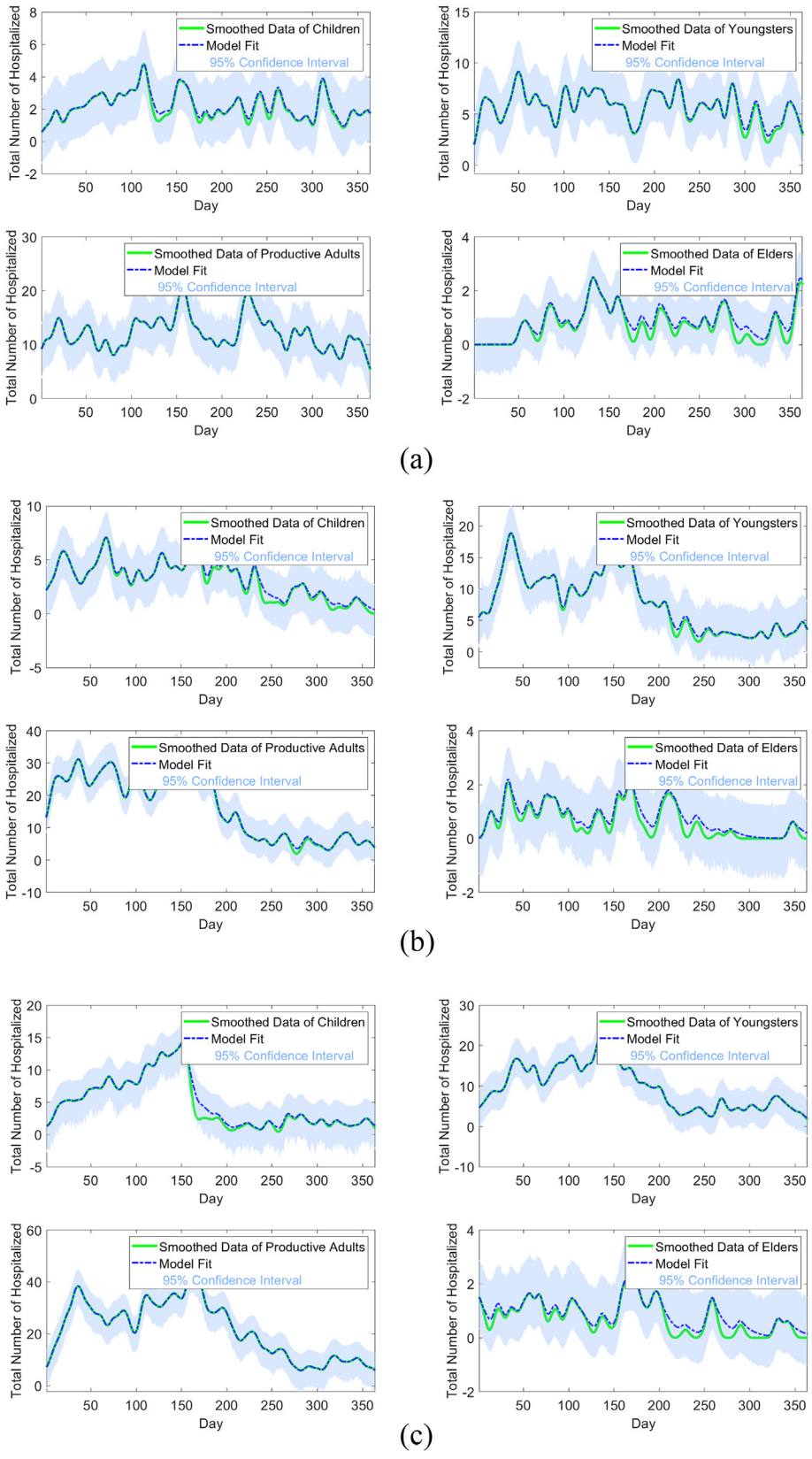

Fig. 3. Fit between the total number of daily hospitalizations (smoothed data) and the age structure model for (a) 2014, (b) 2015, and (c) 2016.

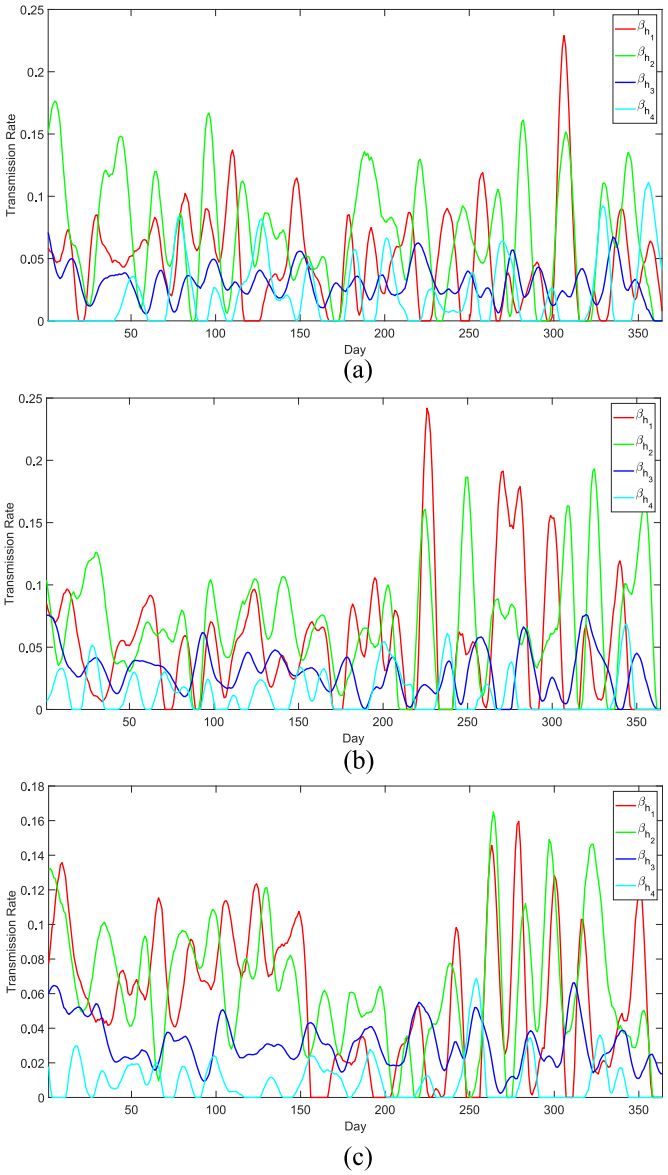

Fig. 4. Time-dependent transmission rates of the age structure model for (a) 2014, (b) 2015, and (c) 2016.

where $\alpha_0 = \alpha_4 = 0$ and $\beta_{h_i}(t)$ are non-negative functions of t. We set the initial condition $S_i(0) = N_{h_i} - I_i(0)$, where N_{h_i} denotes the total population of age structure i, $I_i(0)$ are the first observation data, $R(0) = 0$, and we assume that the total mosquito

Table 3
Sensitivity indices of R_0.

Parameter (k)	Sensitivity Indices (φ_k)		
	2014	**2015**	**2016**
β_{h_1}	+ 0.33859	+ 0.37197	+ 0.38034
β_{h_2}	+ 0.05025	+ 0.04863	+ 0.04400
β_{h_3}	+ 0.05711	+ 0.05307	+ 0.05484
β_{h_4}	+ 0.05405	+ 0.02630	+ 0.02081
β_v	+ 0.50000	+ 0.50000	+ 0.50000
θ_1	− 0.44703	− 0.44655	− 0.44675
θ_2	− 0.15175	− 0.12022	− 0.11242

population is proportional to the total human population. Moreover, we compute the time-dependent effective reproduction ratio in Eq. (10) using the parameter $\beta_{h_i}(t)$, which reflects the effectiveness of the control strategies.

2.2.5. Force of infection in each age-group

We define the annual force of infection (FoI) in each age group as the average rate for a single susceptible individual in each group to get infected. This indicator is formulated as:

$$F_i = \frac{1}{T}\int_0^T \frac{\beta_{h_i}(s) N_v \sum_{j=1}^{4} I_j(s)}{N_h\left(\sum_{j=1}^{4} I_j(s) + \varphi N_h\right)} ds,$$

for $i = 1, 2, 3, 4$. This indicator is good for monitoring the shift in each group's infectivity over different periods (Cummings et al., 2009).

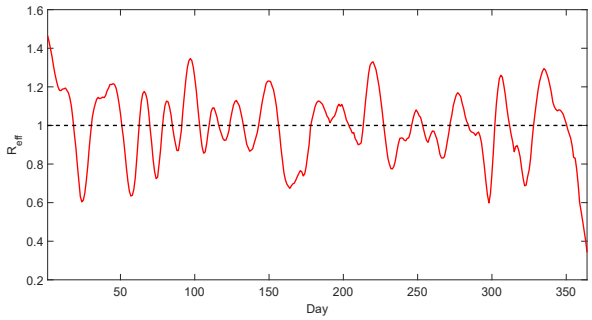

(a)

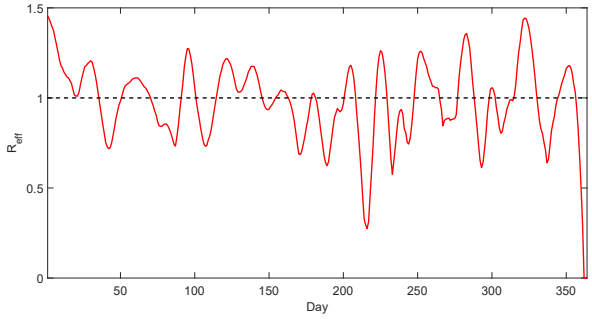

(b)

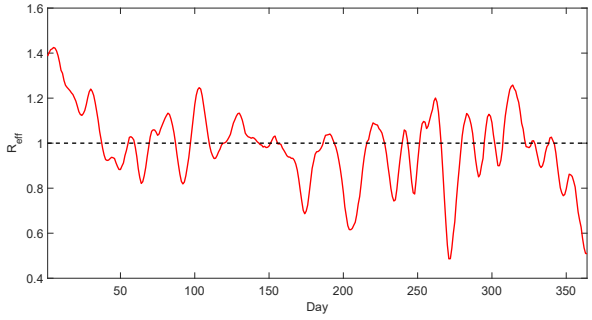

(c)

Fig. 5. Daily effective reproduction ratio for (a) 2014, (b) 2015, and (c) 2016.

3. Results and discussion

We applied the time-dependent model to explain the spread of dengue in Bandung, West Java Province, Indonesia. However, the data used in this study was only a sample of dengue cases in Bandung, thus we assumed that the birth and total human population data in this study were half of the birth and total population in Bandung, respectively (see Table 2). Because the data for each age structure fluctuated highly (see Fig. 1), we did preprocessing on the raw real data by using smoothing method, as in (Demongeot et al., 2020), (Al-Turaiki et al., 2021) and (Zhao et al., 2021). Here, we used the *smoothdata* function with a Gaussian method to smooth the data, as shown in Fig. 3. This daily smoothed data was then used to calculate the daily effective reproduction ratio, $R_{eff}(t)$, with $\theta_1 = \theta_2 = 0$. Hence, one first needs to determine the time-dependent transmission rates, $\beta_{h_i}(t)$, $i = 1 \ldots 4$, for which the time-dependent reduced model has the best agreement with the smoothed data. Since the parameter $\beta_{h_i}(t)$ is non-negative, we set it to 0 if it is less than 0.

Fig. 3 illustrates a simulation made with the time-dependent age structure model and how it fit the data. It can be seen that the time-dependent model had good results in fitting the smoothed data. Here we use time series bootstraps of the residuals from the fitted model to obtain 95% confidence intervals, as in (Carpenter & Bithell, 2000).

In Fig. 4, we show the measured $\beta_{h_i}(t)$, for $i = 1 \ldots 4$ at time t. Furthermore, a sensitivity analysis of R_0 was performed using the parameter values in Table 1 and taking the value of β_{h_i} as the average value of $\beta_{h_i}(t)$. The sensitivity indices of the selected parameters are given in Table 3. We found that the sensitivity index of the transmission rate parameter of the age group of children for every year was greater than the transmission rate parameter for the other age groups, where $\varphi_{\beta_{h_1}} = +\ 0.33859$, which means that increasing (or decreasing) β_{h_1} by 10% will increase (or decrease) R_0 by 3.3859%. Meanwhile, increasing (or decreasing) the vaccination parameter for the age group of children, θ_1, by 10% will decrease (or increase) R_0 by 4.4703%.

The daily effective reproduction ratio for each year obtained using the corresponding $\beta_{h_i}(t)$ is shown in Fig. 5. Note that $R_{eff} = 1$ is the threshold between control of the outbreak is likely ($R_{eff} < 1$) and a sustained infection rate is likely ($R_{eff} > 1$) (Arroyo-Marioli et al., 2021). We can see that the value of the daily effective reproduction ratio fluctuated around the threshold and mostly below the threshold.

The annual force of infection (FoI) for each age group before and after vaccination was also obtained, as presented in Table 4. Ndii et al. (Ndii et al., 2020) state that the efficacy level of a licensed dengue vaccine to reduce dengue transmission is 42–80%. Therefore, for vaccination scenarios, we assumed that vaccines are given to susceptible children or youngsters with a vaccination rate of 1% per day and that vaccine efficacy is 50%. From Table 4, the FoI values for children before vaccination continued to increase from 2014 to 2016, while the reverse held for youngsters. In 2015, the FoI values for children even increased significantly. In addition, the FoI for youngsters was higher than for the other age groups, both before and after vaccination. This indicates that youngsters received intense dengue exposure. Consistent with this, Nealon et al. (Nealon et al., 2020) found that the estimated age at which 80% of children become dengue seropositive was 11 years for Indonesia, and 10 years for West Java. They also reported that the estimated dengue FoI for children aged 1–13 and 14–18 years in Indonesia (West Java) was 15.1% (17%) and 4.1% (−4.6%), respectively, with the age-constant FoI at 14.7% (16.1%). After vaccination, the FoI value declined slightly, but it contributed to a significant decrease in dengue infection, as shown in Figs. 6 and 7. An increase in vaccination rate (η) further decreased the FoI value, see Table 4.

Table 4
Annual force of infection (FoI).

Year	FoI Before Vaccination							
	Children	**Increase/Decrease (%)**	**Youngsters**	**Increase/Decrease (%)**	**Productive Adults**	**Increase/Decrease (%)**	**Elders**	**Increase/Decrease (%)**
2014	0.046720	–	0.067273	–	0.029102	–	0.020571	–
2015	0.051431	10.08	0.065368	−2.83	0.028731	−1.28	0.012125	−41.06
2016	0.054876	6.70	0.061632	−5.72	0.030145	4.92	0.009204	−24.09
Year	**FoI for Vaccinated Children**							
	Children		**Youngsters**		**Productive Adults**		**Elders**	
	$\eta = 0.005$ **(%)**	$\eta = 0.01$ **(%)**	$\eta = 0.005$ **(%)**	$\eta = 0.01$ **(%)**	$\eta = 0.005$ **(%)**	$\eta = 0.01$ **(%)**	$\eta = 0.005$ **(%)**	$\eta = 0.01$ **(%)**
2014	0.046675 (4.67)	0.046645 (4.66)	0.067231 (6.72)	0.067175 (6.72)	0.029076 (2.91)	0.029060 (2.91)	0.020548 (2.05)	0.020534 (2.05)
2015	0.051323 (5.13)	0.051253 (5.13)	0.065248 (6.52)	0.065173 (6.52)	0.028687 (2.87)	0.028659 (2.87)	0.012106 (1.21)	0.012094 (1.21)
2016	0.054826 (5.48)	0.054794 (5.48)	0.061576 (6.16)	0.061542 (6.15)	0.030120 (3.01)	0.030105 (3.01)	0.009197 (0.92)	0.009192 (0.92)
	FoI for Vaccinated Youngsters							
2014	0.046614 (4.66)	0.046540 (4.65)	0.067119 (6.71)	0.067011 (6.70)	0.029036 (2.90)	0.028989 (2.90)	0.020510 (2.05)	0.020469 (2.05)
2015	0.051260 (5.13)	0.051146 (5.11)	0.065117 (6.51)	0.064951 (6.50)	0.028638 (2.86)	0.028576 (2.86)	0.012094 (1.21)	0.012073 (1.21)
2016	0.054771 (5.48)	0.054700 (5.47)	0.061501 (6.15)	0.061414 (6.14)	0.030088 (3.01)	0.030050 (3.01)	0.009187 (0.92)	0.009175 (0.92)

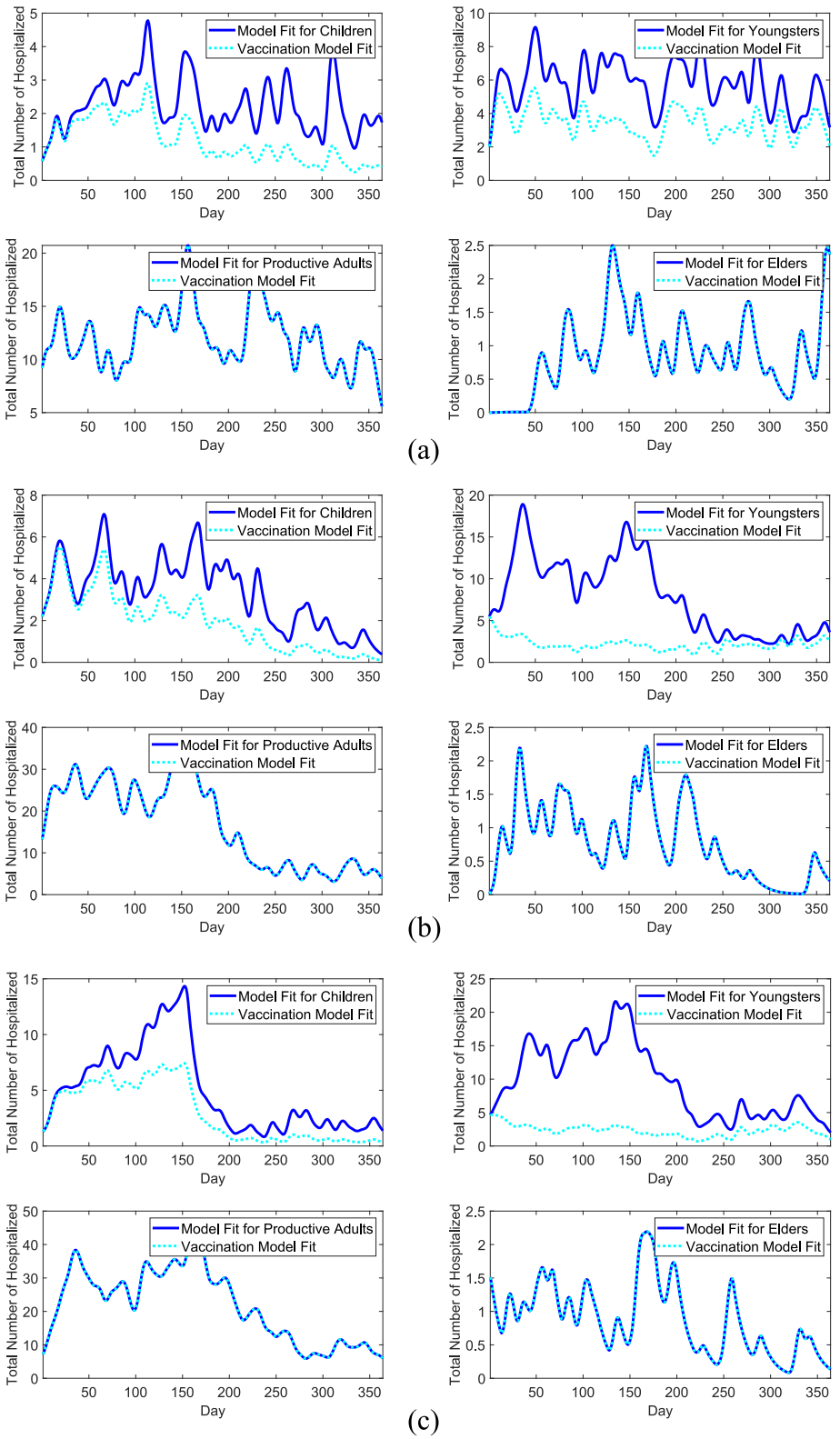

Fig. 6. Dynamics of infected humans for time-dependent age structure model with vaccinated children ($\eta = 0.01$) in (a) 2014, (b) 2015, and (c) 2016.

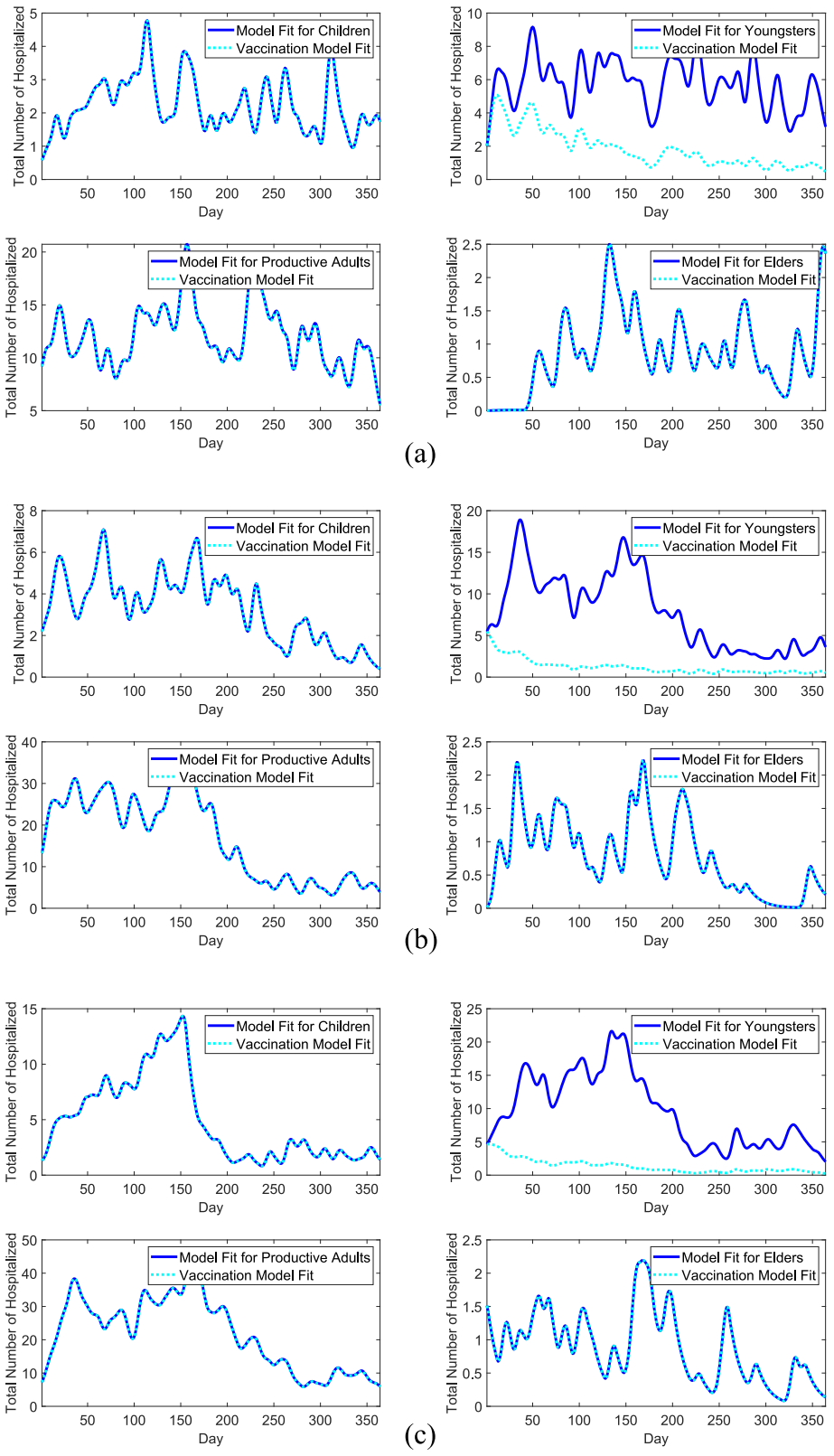

Fig. 7. Dynamics of infected humans for time-dependent age structure model with vaccinated youngsters ($\eta = 0.01$) in (a) 2014, (b) 2015, and (c) 2016.

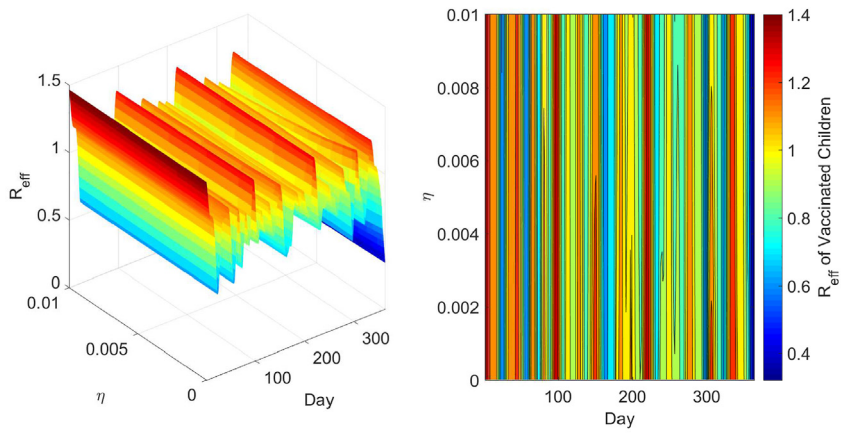

(a)

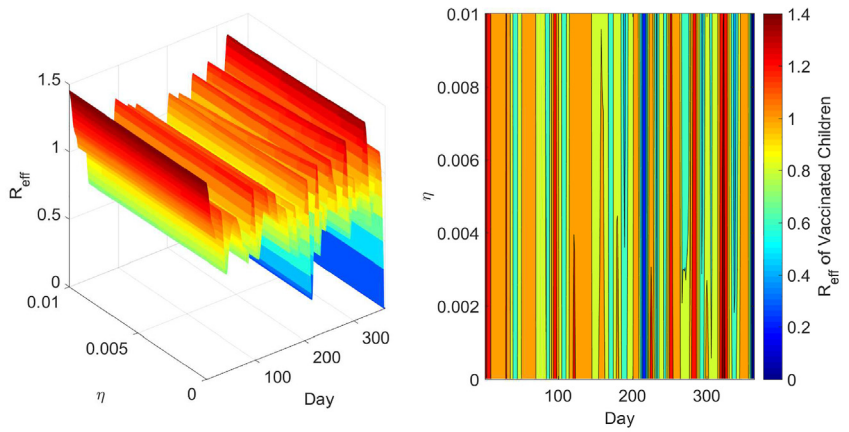

(b)

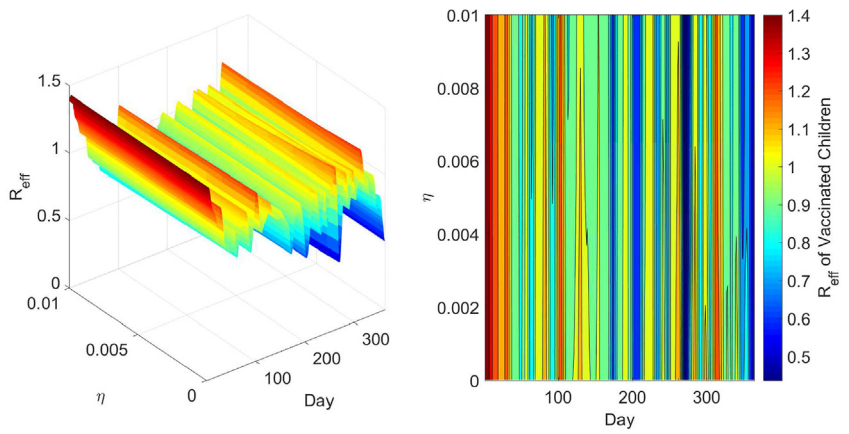

(c)

Fig. 8. Daily effective reproduction ratio for vaccinated children in (a) 2014, (b) 2015, and (c) 2016.

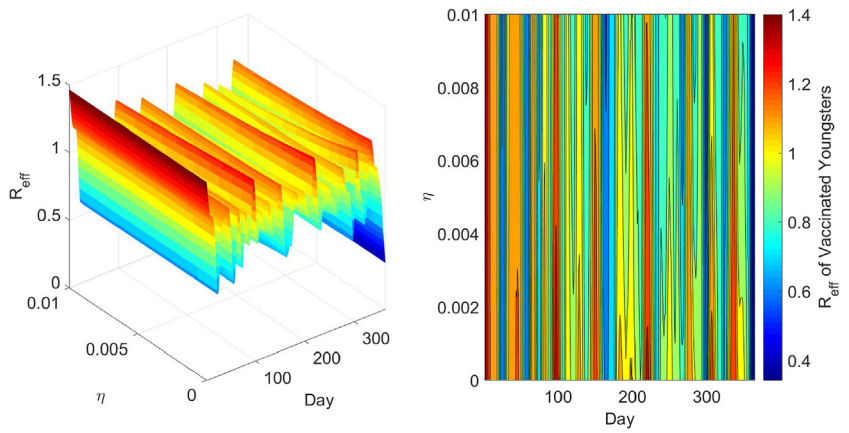

(a)

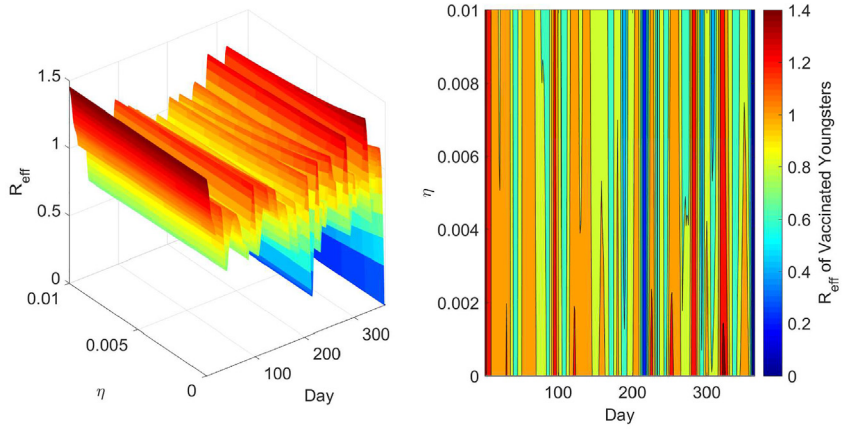

(b)

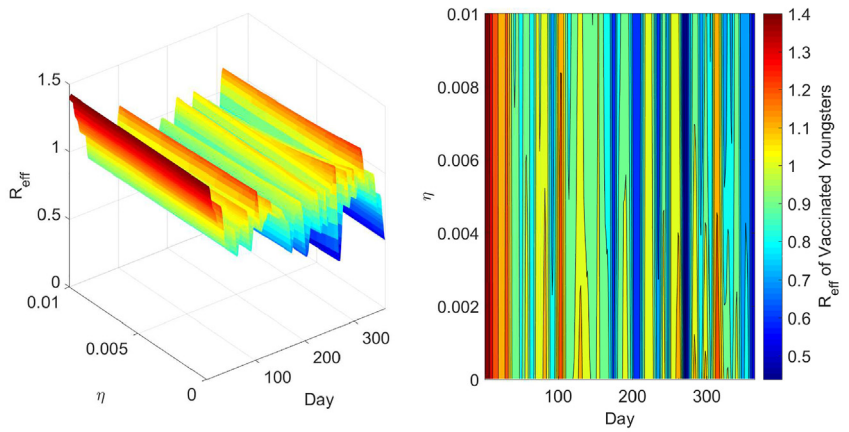

(c)

Fig. 9. Daily effective reproduction ratio for vaccinated youngsters in (a) 2014, (b) 2015, and (c) 2016.

Furthermore, we used the values of parameter $\beta_{h_i}(t)$, for $i = 1 \ldots 4$ generated by the numerical simulation to compute the value of the daily effective reproduction ratio for vaccinated children and vaccinated youngsters, respectively. Assuming that vaccination is given up to 1% per day, with 50% vaccine efficacy, we obtained the daily effective reproduction ratio as shown in Figs. 8 and 9.

Figs. 8 and 9 present the daily effective reproduction ratio for vaccinated children and vaccinated youngsters, respectively, from 2014 to 2016. From the two figures, it can be seen that the daily effective reproduction ratio declined slowly when the vaccination rate was increased. Furthermore, note that vaccination of youngsters caused the effective reproduction ratio to decrease more rapidly than vaccination of children. This shows that vaccination of youngsters is the best control strategy to reduce the spread of dengue.

4. Conclusions

We constructed a time-dependent age structure model with vaccination to explore the dengue transmission dynamics in Bandung city based on daily dengue incidence. The time-dependent model fit well with the incidence data, from which daily transmitting rates were obtained. The time-dependent transmission rates for each age group obtained were used to compute the daily effective reproduction ratio as a daily threshold parameter to assess the effectiveness of vaccination in one of the age groups. Furthermore, the annual force of infection (FoI) for each age group, both before and after vaccination, was calculated to determine the dengue transmission intensity for each age group. The highest dengue transmission intensity was observed in the youngster group, both before and after vaccination. After vaccination, there was a relatively small decrease in the force of infection, but it resulted in a significant decline in annual dengue cases. In addition, we found that vaccination of youngsters had the most significant impact on reducing annual dengue cases in Bandung city based on the daily effective reproduction ratio. Limitations of this study include the assumption of population homogeneity, the number of the population of each age group being assumed to be constant over time and other assumptions used in the model and simulation, as well as other factors that were not involved.

CRediT authorship contribution

Juni Wijayanti Puspita: Conceptualization, Formal analysis, Methodology, Software, Writing – review & editing. **Muhammad Fakhruddin:** Methodology, Validation, Writing – review & editing. **Nuning Nuraini:** Conceptualization, Supervision, Validation. **Edy Soewono:** Conceptualization, Supervision, Writing – review & editing.

Funding

Part of the research is funded by the Indonesian PDUPT RistekBrin 2021 (No: 120M/IT1.C02/TA.00/2021), and the Indonesian Penelitian Disertasi Doktor RistekBrin 2021 (No: 120J/IT1.C02/TA.00/2021).

Declaration of competing interest

The authors declare that they have no known competing financial interests or personal relationships that could have appeared to influence the work reported in this paper.

Acknowledgements

Thanks to Santo Borromeus Hospital Bandung, Indonesia for providing the dengue case data. We also thank Afrina Andriani Sebayang for suggestions and useful discussions.

References

Aguiar, M., Mateus, L., & Stollenwerk, N. (2016a). The currently best estimate for worldwide dengue vaccine efficacy. In *AIP conference proceedings* (Vol. 1738) AIP Publishing LLC, Article 390014.

Aguiar, M., & Stollenwerk, N. (2018). Dengvaxia: Age as surrogate for serostatus. *The Lancet Infectious Diseases, 18*, 245.

Aguiar, M., Stollenwerk, N., & Halstead, S. B. (2016b). The impact of the newly licensed dengue vaccine in endemic countries. *PLoS Neglected Tropical Diseases, 10*, Article e0005179.

Al-Turaiki, I., Almutlaq, F., Alrasheed, H., & Alballa, N. (2021). Empirical evaluation of alternative time-series models for covid-19 forecasting in Saudi Arabia. *International Journal of Environmental Research and Public Health, 18*, 8660.

Arroyo-Marioli, F., Bullano, F., Kucinskas, S., & Rondón-Moreno, C. (2021). Tracking r of covid-19: A new real-time estimation using the kalman filter. *PLoS One, 16*, Article e0244474.

Bandung, B. P. S. K. (2015). *Kota bandung dalam angka 2015. Retrieved from* http://bandungkota.bps.go.id/publikasi/kota-bandung-dalam-angka.

Bandung, B. P. S. K. (2016). *Kota bandung dalam angka 2016. Retrieved from* http://bandungkota.bps.go.id/publikasi/kota-bandung-dalam-angka.

Bandung, B. P. S. K. (2017). *Kota bandung dalam angka 2017. Retrieved from* http://bandungkota.bps.go.id/publikasi/kota-bandung-dalam-angka.

Biswal, S., Reynales, H., Saez-Llorens, X., Lopez, P., Borja-Tabora, C., Kosalaraksa, P., Sirivichayakul, C., Watanaveeradej, V., Rivera, L., Espinoza, F., et al. (2019). Efficacy of a tetravalent dengue vaccine in healthy children and adolescents. *New England Journal of Medicine, 381*, 2009–2019.

Bustamam, A., Aldila, D., & Yuwanda, A. (2018). Understanding dengue control for short-and long-term intervention with a mathematical model approach. *Journal of Applied Mathematics, 2018*, 1–13, 9674138.

Carpenter, J., & Bithell, J. (2000). Bootstrap confidence intervals: When, which, what? A practical guide for medical statisticians. *Statistics in Medicine, 19*, 1141–1164.
Chen, Y. C., Lu, P. E., Chang, C. S., & Liu, T. H. (2020). *A time-dependent sir model for covid-19 with undetectable infected persons*. IEEE Transactions on Network Science and Engineering.
CNN-Indonesia ( ). Kasus corona kota bandung stagnan, wabah dbd meningkat. URL: https://www.cnnindonesia.com/nasional/20200624162839-20-517032/kasus-corona-kota-bandung-stagnan-wabah-dbd-meningkat.
Cummings, D. A., Iamsirithaworn, S., Lessler, J. T., McDermott, A., Prasanthong, R., Nisalak, A., et al. (2009). The impact of the demographic transition on dengue in Thailand: Insights from a statistical analysis and mathematical modeling. *PLoS Medicine, 6*, Article e1000139.
Demongeot, J., Griette, Q., & Magal, P. (2020). *Si epidemic model applied to covid-19 data in mainland China* (Vol. 7). Royal Society open science, Article 201878.
Diekmann, O., Heesterbeek, J., & Roberts, M. G. (2010). The construction of next-generation matrices for compartmental epidemic models. *Journal of The Royal Society Interface, 7*, 873–885.
Duijzer, E., van Jaarsveld, W., Wallinga, J., & Dekker, R. (2016). The most efficient critical vaccination coverage and its equivalence with maximizing the herd effect. *Mathematical Biosciences, 282*, 68–81.
Egger, J. R., & Coleman, P. G. (2007). Age and clinical dengue illness. *Emerging Infectious Diseases, 13*, 924.
Esteva, L., & Vargas, C. (1998). Analysis of a dengue disease transmission model. *Mathematical Biosciences, 150*, 131–151.
Fauzi, I. S., Fakhruddin, M., Nuraini, N., & Wijaya, K. P. (2019). Comparison of dengue transmission in lowland and highland area: Case study in semarang and malang, Indonesia. *Communication in Biomathematical Sciences, 2*, 23–37.
Götz, T., Altmeier, N., Bock, W., Rockenfeller, R., Sutimin, & Wijaya, K. P. (2017). Modeling dengue data from semarang, Indonesia. *Ecological Complexity, 30*, 57–62.
Jan, R., & Xiao, Y. (2019). Effect of pulse vaccination on dynamics of dengue with periodic transmission functions. *Advances in Difference Equations*, 1–17, 2019.
Kabir, K. A., & Tanimoto, J. (2020). Cost-efficiency analysis of voluntary vaccination against n-serovar diseases using antibody-dependent enhancement: A game approach. *Journal of Theoretical Biology, 503*, Article 110379.
Karyanti, M. R., Uiterwaal, C. S., Kusriastuti, R., Hadinegoro, S. R., Rovers, M. M., Heesterbeek, H., et al. (2014). The changing incidence of dengue haemorrhagic fever in Indonesia: A 45-year registry-based analysis. *BMC Infectious Diseases, 14*, 1–7.
Musa, S. S., Hussaini, N., Zhao, S., & Daihai, H. (2020). Dynamical analysis of chikungunya and dengue co-infection model. *Discrete & Continuous Dynamical Systems-B, 25*, 1907.
Mustafa, M., Rasotgi, V., Jain, S., & Gupta, V. (2015). Discovery of fifth serotype of dengue virus (denv-5): A new public health dilemma in dengue control. *Medical Journal Armed Forces India, 71*, 67–70.
Ndii, M. Z., Mage, A. R., Messakh, J. J., & Djahi, B. S. (2020). Optimal vaccination strategy for dengue transmission in kupang city, Indonesia. *Heliyon, 6*, Article e05345.
Nealon, J., Bouckenooghe, A., Cortes, M., Coudeville, L., Frago, C., Macina, D., et al. (2020). *Dengue endemicity, force of infection and variation in transmission intensity in 13 endemic countries*. The Journal of infectious diseases.
Polwiang, S. (2016). Vaccine coverage and the cost effectiveness of dengue vaccine in south east asia. *PeerJ PrePrints, 4*, Article e1694v1.
Prayitno, A., Taurel, A. F., Nealon, J., Satari, H. I., Karyanti, M. R., Sekartini, R., et al. (2017). Dengue seroprevalence and force of primary infection in a representative population of urban dwelling Indonesian children. *PLoS Neglected Tropical Diseases, 11*, Article e0005621.
Sasmono, R. T., Taurel, A. F., Prayitno, A., Sitompul, H., Yohan, B., Hayati, R. F., et al. (2018). Dengue virus serotype distribution based on serological evidence in pediatric urban population in Indonesia. *PLoS Neglected Tropical Diseases, 12*, Article e0006616.
Shim, E. (2016). Dengue dynamics and vaccine cost-effectiveness analysis in the Philippines. *The American Journal of Tropical Medicine and Hygiene, 95*, 1137.
Shim, E. (2017). Cost-effectiveness of dengue vaccination in yucatán, Mexico using a dynamic dengue transmission model. *PLoS One, 12*, Article e0175020.
Shim, E. (2019). Optimal dengue vaccination strategies of seropositive individuals. *Mathematical Biosciences and Engineering, 16*, 1171–1189.
Supriatna, A., Soewono, E., & van Gils, S. A. (2008). A two-age-classes dengue transmission model. *Mathematical Biosciences, 216*, 114–121.
Tam, C. C., O'Driscoll, M., Taurel, A. F., Nealon, J., & Hadinegoro, S. R. (2018). Geographic variation in dengue seroprevalence and force of infection in the urban paediatric population of Indonesia. *PLoS Neglected Tropical Diseases, 12*, Article e0006932.
Tang, X., Zhao, S., Chiu, A. P., Wang, X., Yang, L., & He, D. (2017). Analysing increasing trends of guillain-barré syndrome (gbs) and dengue cases in Hong Kong using meteorological data. *PLoS One, 12*, Article e0187830.
Tay, C. J., Fakhruddin, M., Fauzi, I. S., Teh, S. Y., Syamsuddin, M., Nuraini, N., & Soewono, E. (2022). Dengue epidemiological characteristic in kuala lumpur and selangor, Malaysia. *Mathematics and Computers in Simulation, 194*, 489–504.
Thai, K. T., Nishiura, H., Hoang, P. L., Tran, N. T. T., Phan, G. T., Le, H. Q., Tran, B. Q., Nguyen, N. V., & de Vries, P. J. (2011). Age-specificity of clinical dengue during primary and secondary infections. *PLoS Neglected Tropical Diseases, 5*, Article e1180.
Thomas, S. J., & Yoon, I. K. (2019). A review of dengvaxia®: Development to deployment. *Human Vaccines & Immunotherapeutics, 15*, 2295–2314.
Van den Driessche, P. (2017). Reproduction numbers of infectious disease models. *Infectious Disease Modelling, 2*, 288–303.
Yip, S., Him, N. C., Jamil, N. I., He, D., & Sahu, S. K. (2022). Spatio-temporal detection for dengue outbreaks in the central region of Malaysia using climatic drivers at mesoscale and synoptic scale. *Climate Risk Management, 36*, Article 100429.
Zeng, W., Halasa-Rappel, Y. A., Baurin, N., Coudeville, L., & Shepard, D. S. (2018). Cost-effectiveness of dengue vaccination in ten endemic countries. *Vaccine, 36*, 413–420.
Zhao, H., Merchant, N. N., McNulty, A., Radcliff, T. A., Cote, M. J., Fischer, R. S., Sang, H., & Ory, M. G. (2021). Covid-19: Short term prediction model using daily incidence data. *PLoS One, 16*, Article e0250110.
Zhao, S., Musa, S. S., Hebert, J. T., Cao, P., Ran, J., Meng, J., He, D., & Qin, J. (2020). Modelling the effective reproduction number of vector-borne diseases: The yellow fever outbreak in luanda, angola 2015–2016 as an example. *PeerJ, 8*, Article e8601.